Heterogeneous Catalysis

DOI: 10.1002/ange.200601853

Single Gold Atoms in Heterogeneous Catalysis: Selective 1,3-Butadiene Hydrogenation over Au/ZrO_2**

Zhi-Pan Liu, Chuan-Ming Wang, and Kang-Nian Fan*

Oxide-supported metal systems are perhaps the most common heterogeneous catalysts, in which metal particles are long believed to be responsible for the catalytic activity.[1] This general concept is, however, challenged by recent studies, particularly on Au-based catalysts.[2–6] It was reported that single Au atoms/cations supported on certain oxides can catalyze reactions such as CO oxidation,[3] the water gas shift reaction ($CO + H_2O$),[4] and hydrogenation.[5,6] These findings imply the cost of noble-metal catalysts may be decreased dramatically and homogeneous catalysis may be mimicked in a heterogeneous environment if metal cations are highly dispersed on oxides. Such a linkage between heterogeneous and homogeneous catalysis, if established, is of huge incentive.[2] Although homogeneous catalysis by cationic gold has been well documented,[7,8] their heterogeneous analogues are newly identified and many fundamental issues are illusive, such as the active-site structure, the oxidation state of Au, and the microscopic reaction mechanism. Our aim is to provide deeper insight into the single Au heterogeneous catalysis; therefore, the selective hydrogenation of 1,3-butadiene ($H_2C{=}HC\text{-}HC{=}CH_2$) on Au/ZrO_2 is studied herein as a model reaction using density functional theory (DFT) slab calculations.

The activity of Au complexes deposited on various oxides, such as La_2O_3,[3a] MgO,[5a] zeolite NaY,[3b] ceria,[4] and zirconia,[6] has been tested over recent years in investigations into the possibility of performing homogeneous catalytic reactions under heterogeneous conditions. In particular, Zhang et al.[6] reported that the Au/ZrO_2 catalyst remains highly active at very low loadings of Au for the hydrogenation of 1,3-butadiene and that butene is selectively produced without any butane by-product. The Au species in the catalyst was found to be Au^{III} by using X-ray photoelectron spectroscopy (XPS) and H_2 titration. The high selectivity is rather surprising as 1,3-butadiene hydrogenation is conventionally catalyzed by precious transition metals (Pd, Pt), in which the deep hydrogenation to butane is a known problem. It is therefore highly desirable to understand the origin of this single Au heterogeneous catalysis by comparing it with traditional heterogeneous catalysis on metal particles and also with Au-based homogeneous catalysis.

Knowledge of how Au monomers bind to ZrO_2 is the first step towards a systematic understanding of the selective butadiene hydrogenation. We considered four possible Au monomers on zirconia, namely, Au atom (Au^0), AuOH (Au^I), AuOOH, and $Au(OH)_3$ (Au^{III}) for this purpose. Tetragonal ZrO_2 (t-ZrO_2) was chosen as the support because it is one of the common phases in the prepared ZrO_2.[9] Both flat and stepped t-ZrO_2 surfaces were then used to anchor the four Au monomers (ZrO_2 can hardly be reduced,[10] and thus surface O vacancies were not considered). The modeled flat t-ZrO_2 surface is the most stable surface (that is, the flat t-ZrO_2{101} as shown in Figure 1a,b). In addition, two types of stepped surfaces, {001}- and {100}-type, which can be naturally cleaved from the t-ZrO_2{101} surface are modeled, as represented by the low Miller index surfaces, {203} and {201}, respectively (Figure 1c,d). The {001}- and {100}-type steps are expected to be the most common structural defects in t-ZrO_2 because the {001} and {100} surfaces of t-ZrO_2 are more stable than any other surface planes, except for the most stable {101} surface.[10b] All DFT slab calculations were performed using

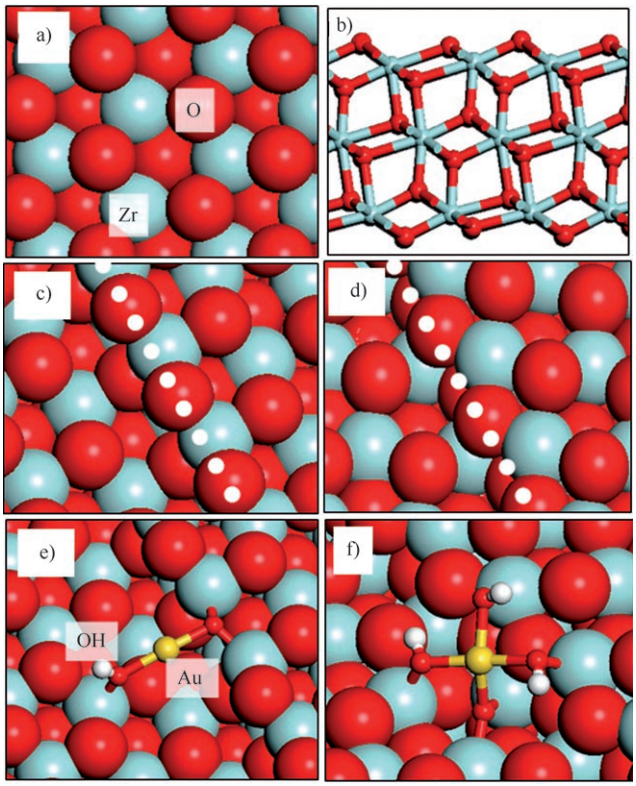

Figure 1. The modeled surface structures and the structures of the cationic Au monomer adsorption at the steps (O red, Zr blue, Au yellow, H gray). a,b) Top and side views, respectively, of t-ZrO_2{101}; c) t-ZrO_2{203} with {001}-type steps; d) t-ZrO_2{201} with {100}-type steps; e) AuOH/t-ZrO_2{203}; and f) $Au(OH)_3$/t-ZrO_2{201}. The dotted lines in (c) and (d) are drawn along the step edges to guide the eye.

[*] Prof. Z.-P. Liu, C.-M. Wang, Prof. K.-N. Fan
Shanghai Key Laboratory of Molecular Catalysis and Innovative Materials
Department of Chemistry, Fudan University
Shanghai 200433 (China)
Fax: (+86) 21-6564-2400
E-mail: zpliu@fudan.edu.cn

[**] This work was supported by the NSF of China (20573023, 20433020), Pujiang Plan, and NSF of Shanghai Sci. Tech. Committee (06PJ14011, 02JD14023, and 05DZ22313). The authors thank the Shanghai Supercomputing Center for computing time.

Supporting information for this article is available on the WWW under http://www.angewandte.org or from the author.

the SIESTA package with a GGA-PBE functional (see Supporting Information for calculation details).[11,12]

The adsorption of the four Au monomers on the t-ZrO_2 surfaces were investigated first. The structures were checked with Nose thermostat molecular dynamics at 300 K to avoid trapping in local minima. We measured the thermodynamic stability of the Au monomers by using the reaction shown as Equation (1), in which Au(X) represents the four Au monomers (see Table 1) and y and z are coefficients to balance the reaction.

$$Au(OH)_3 + ZrO_2 \rightarrow [Au(X)]/ZrO_2 + y\,H_2O + z\,O_2 \quad (1)$$

The reaction describes the formation of the Au/ZrO_2 catalyst starting from the Au^{III}-containing solution ($HAuCl_4$ in alkaline solutions), which then undergoes calcination at 473 K in the experimental investigation.[6] The calculated reaction energies ΔE_f of the most stable Au(X) monomer are listed in Table 1 (the calculated Au–O bond lengths are listed in the Supporting Information). The ΔE_f values were obtained directly from the DFT total energy (E is, strictly speaking, the Helmohotz free energy at 0 K with zero-point vibrations being neglected). For solid states, such as ZrO_2 and Au(X)/ZrO_2 in Equation (1), this is a good approximation to the Gibbs free energy (G) as the temperature T and pressure p contributions are small. The E values for gas-phase molecules can be quite different from the G values, mainly as a result of the large entropy term at elevated temperatures.[13,14] Herein, we utilize standard thermodynamic data to estimate the temperature contribution to the free energy of gas-phase H_2O and O_2 following the procedure as described previously.[14] Our calculations showed that for 1 mol O_2 at (500 K, 1 atm), $G(O_2)$ is lower than $E(O_2)$ (with zero-point energy included) by 0.93 eV, whereas it is 0.89 eV for H_2O. Then, the ΔG_f values at 500 K/1 atm for the formation of the Au monomers could be estimated (Table 1).

Table 1: The reaction energies (ΔE_f) and reaction free energies (ΔG_f; 500 K, 1 atm) of Au monomers (Au(X)) deposited on the flat {101}, stepped {203}, and {201} t-ZrO_2 surfaces.

Au(X)	{101}		{203}		{201}	
	ΔE_f [eV]	ΔG_f [eV]	ΔE_f [eV]	ΔG_f [eV]	ΔE_f [eV]	ΔG_f [eV]
$Au(OH)_3$	−2.64	−2.64	−3.23	−3.23	−3.66	−3.66
AuO_2H	−1.35	−2.25	−1.61	−2.51	−1.53	−2.43
AuOH	−1.76	−3.12	−2.33	−3.69	−1.94	−3.30
Au	0.03	−2.00	0.53	−1.51	0.45	−1.59

It can be seen from Table 1 that the $Au(OH)_3$ moieties (Au^{III}) at the oxide defects are the most stable of the four different Au monomers at low temperatures, whereas the neutral Au^0 atoms adsorb most weakly on all ZrO_2 surfaces. This result agrees with the experimental evidence for the presence of Au^{III}.[3,6] Another stable Au species is Au^I, whose stability quickly "catches up" as the temperature increases. Au^I on the flat {101} and stepped {203} surfaces at 500 K are already more stable than Au^{III}. By further considering the formation of Au metal starting from $Au(OH)_3$, that is, $Au(OH)_3 \rightarrow Au^0$ atom $\rightarrow$ Au bulk, we can deduce that the ΔE_f value for the formation of bulk Au is approximately −3 eV (Au cohesive energy is −3.2 eV from our DFT studies). As metallic Au is also less stable than $Au(OH)_3$ on ZrO_2, we can conclude that Au^{III} on ZrO_2 is the most stable Au species at low temperatures (e.g., below 500 K). The entropy terms of the decomposition products, H_2O and O_2, will shift the equilibrium towards the reduced form of Au at high temperatures and finally lead to bulk Au.

Table 1 also shows that relative to the flat {101} surface, generally stepped sites can stabilize ionic Au monomers (Au^I and Au^{III}) better. But, why? On metal surfaces, it is well known that defects bond to many adsorbates more strongly as a result of the metal atom being less coordinated with more reactive d states.[12b,14] However, we found that the physical origin of the enhanced bonding for ionic Au at oxide defects is quite different. We have illustrated the structure of the two most stable ionic Au species, that is, AuOH/t-ZrO_2{203} and $Au(OH)_3$/t-ZrO_2{201} in Figure 1e,f. Similar to the structure of cationic Au in solution,[7,8] our results show that the most stable Au^I center has a two-coordinate linear structure (Figure 1e) and Au^{III} has a four-coordinate planar structure (Figure 1f). Such saturated Au monomers are generally more stable than unsaturated ones. Clearly, to achieve the particular structure for Au, a suitable local geometry is required for lattice O atoms (O_{latt}) that surround the Au cation, and the OH groups attached to the Au center should be stabilized by Zr cations. This behavior leads to the formation of Au-O-Zr linkages. At defected sites of the oxide, it is more convenient to achieve the linear or planar structure for ionic Au. By contrast, the flat {101} surface has to undergo significant relaxation to achieve the Au linear or planar structure. Thus, the Au cations there are generally less stable.

As the hydrogenation of 1,3-butadiene is performed under reductive conditions at 400 K, one may argue that the oxidized form Au^{III} may not be stable for this reaction. We analyzed the possibility of Au^I formation from Au^{III} from thermodynamic data by using the chemical formula shown in Equation (2).

$$Au(OH)_3/ZrO_2 + H_2 \rightarrow AuOH/ZrO_2 + 2\,H_2O \quad (2)$$

On the basis of the data in Table 1, we calculated that the ΔE_f values of the reaction [Eq. (2)] are −1.58, −1.55, and −0.74 eV for the flat and stepped surfaces, respectively. As all the values are negative, it is indicated that the $Au^{III} \rightarrow Au^I$ reduction is thermodynamically favored. In addition, we further checked the kinetic possibility of H_2 dissociation on Au^{III} at the reaction temperature (400 K). As a representative, we examined the transition state for H_2 dissociations on $Au(OH)_3$ at the stepped {201} surface, in which the ΔE_f value of $Au^{III} \rightarrow Au^I$ is the highest. The reaction barrier is calculated to be only 0.16 eV. Therefore, both the thermodynamic and kinetic data indicate that the $Au^{III} \rightarrow Au^I$ conversion under these reaction conditions is allowed. By considering that Au^I may already be produced at the calcination stage on the {101} and {001} steps, it is expected that Au^I is the dominant Au species under the reaction conditions instead of Au^{III}.

To shed light on the Au^I-catalyzed hydrogenation of 1,3-butadiene, we studied the reaction on the AuOH/t-ZrO_2{203}

surface, in which AuOH is the most stable Au^I species (Table 1). AuOH attaches to the {001} step through an Au–O_{latt} bond and HO–Zr bond, in which the O_{latt} atom is a step-edge lattice O atom and the Zr atom is located on the {101} terrace (Figure 1e). The reaction pathways and the reaction barriers were determined, as shown in the reaction profile in Figure 2.

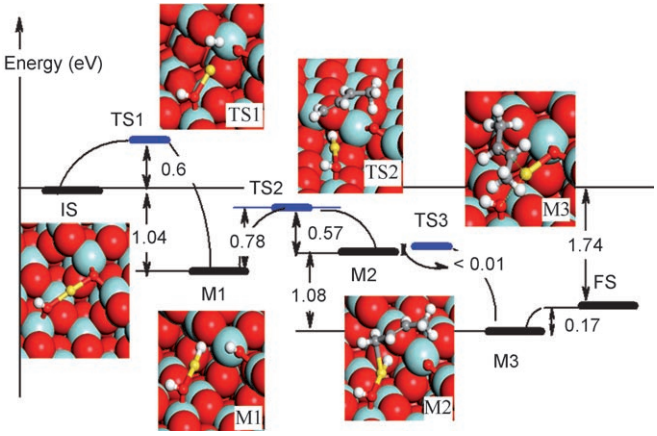

Figure 2. The overall energy profile and reaction snapshots for 1,3-butadiene hydrogenation (formation of butene) on the AuOH/t-ZrO_2-{203} surface. IS = initial state, FS = final state, M = intermediate state, and TS = transition state.

This lowest energy reaction pathway is described as follows. 1) Heterolytic H_2 dissociation: As H_2 approaches AuOH, the Au–O_{latt} bond must break to dissociate H_2 (TS1 in Figure 2), thus leading to H–AuOH and HO_{latt} species (M1 in Figure 2). Mulliken charge analysis of the dissociated product showed that the two dissociated H species are quite different in nature: the one at the O_{latt} atom is protonlike (charge: +0.34), whereas the H species at the Au center is negatively charged (−0.01) and hydridelike. This behavior indicates that H_2 dissociation at Au^I belongs to heterolytic dissociation. It was also noticed that after H_2 dissociation, the charge on the Au center is reduced remarkably from +0.42 to +0.01.

2) Hydrogenation of 1,3-butadiene: 1,3-Butadiene (C_4H_6) could react with either the H–AuOH or HO_{latt} species. As 1,3-butadiene only weakly adsorbs on the surface (below 0.2 eV), the initial state of butadiene is considered to be a gas-phase molecule. Among the two possibilities of H addition, we found that butadiene cannot react with the hydride, but can react with the proton of HO_{latt}. In searching for the hydride reaction pathway, we found that the structural optimization of the hydrogenated intermediate (C_4H_7) is not stable and can spontaneously transform back to the initial state, H-Au-OH, and 1,3-butadiene. This finding may not be surprising as butadiene is a nucleophilic molecule that does not tend to react with a negative hydride species. On the other hand, for butadiene to react with the proton at the O_{latt} atom, a transition state (Figure 2, TS2) can be located when the distance between H and O_{latt} is 1.40 Å and that between C and H is 1.31 Å. The calculated reaction barrier of this step is 0.78 eV. After the TS, the newly formed C_4H_7 adsorbs at the Au center to form a metastable state M2, H-Au-(C_4H_7)OH (Figure 2). This metastable state can readily undergo intermolecular rearrangement by passing the hydride to the adsorbed C_4H_7 species to finally yield adsorbed butene (Figure 2, M3). The final desorption of butene requires 0.17 eV.

It is of interest to ask whether the deep-hydrogenation process, that is, the conversion of butene into butane (C_4H_{10}), can occur. Clearly, the deep hydrogenation (if having taken place) is a secondary process: the newly formed butene at one Au site can only be hydrogenated at a second Au site. Following this process, we identified a pathway for butene → butane conversion, which is very similar to that for butadiene → butene (see Supporting Information for details). The highest barrier (0.82 eV) occurs also at the first hydrogenation step (butene reacts with HO_{latt}). On the basis of these findings, we suggest that the lack of a deep-hydrogenation product in the experimental investigation[6] cannot be justified by energetics. Instead, we may understand it by the following: First, the secondary process is intrinsically slow and the resulting butene needs to compete with butadiene for hydrogenation reaction sites. Second, the butene when produced will desorb as a "hot" molecule, as a result of the large exothermicity of the hydrogenation (Figure 1). Because of the high kinetic energy of butene, the deep hydrogenation that requires the gas-phase butene to react directly with the HO_{latt} species of an Au site (Eley–Rideal mechanism) becomes kinetically unlikely, as our calculations show that the correct geometry for butene in the approach to HO_{latt} is crucial. Consistent with our suggestions, we noticed that ethene → ethane has been observed on cationic Au supported on MgO.[5]

We are now in the position to compare the single Au heterogeneous catalysts with their homogeneous analogues. As mentioned, the oxide enables AuOH to achieve a two-coordinate linear structure, and the Au–O_{latt} bond must break to form free two sites to accommodate two H species (Figure 2, M1).[15] During the hydrogenation process, the linear structure of Au^I is conserved (see Figure 2). This mechanism is rather striking, as the Au^I on the oxide shows the similar ligand attacking/leaving chemistry as those that usually occur in homogeneous catalysis. It should also be emphasized that although ZrO_2 does play an important role in the stabilization of cationic Au, it is not merely a support. As the lattice O atom of ZrO_2 attracts the proton from H_2, it acts as a base to provide additional reaction sites. This behavior implies that oxides with strong acid–base pairs may enhance the catalyst activity.

In summary, our structures of Au cationic monomers on ZrO_2 show a clear resemblance to those in solution. We found that Au^I on ZrO_2 is the catalytically active species that is produced from Au^{III} in situ by reduction. The catalytic roles of the oxide defects and the dynamic ligand effect in reactions have been highlighted. It is shown that in single Au heterogeneous catalysis, the oxide not only stabilizes Au monomers as the solution does in homogeneous catalysis but can also act as a catalyst by providing additional reaction sites.

Received: May 11, 2006
Revised: July 1, 2006
Published online: September 25, 2006

Keywords: density functional calculations · gold · heterogeneous catalysis · hydrogenation

[1] a) M. Haruta, *Catal. Today* **1997**, *36*, 153; b) G. C. Bond, D. T. Thompson, *Catal. Rev. Sci. Eng.* **1999**, *41*, 319.
[2] a) J. M. Thomas, R. Raja, D. W. Lewis, *Angew. Chem.* **2005**, *117*, 6614; *Angew. Chem. Int. Ed.* **2005**, *44*, 6456; b) D. K. Böhme, H. Schwarz, *Angew. Chem.* **2005**, *117*, 2388; *Angew. Chem. Int. Ed.* **2005**, *44*, 2336.
[3] a) J. C. Fierro-Gonzalez, V. A. Bhirud, B. C. Gates, *Chem. Commun.* **2005**, 5275; b) J. C. Fierro-Gonzalez, B. C. Gates, *J. Phys. Chem. B* **2004**, *108*, 16999.
[4] a) Q. Fu, H. Saltsburg, M. Flytzani-Stephanopoulos, *Science* **2003**, *301*, 935; b) Z. P. Liu, S. J. Jenkins, D. A. King, *Phys. Rev. Lett.* **2005**, *94*, 196102.
[5] a) J. Guzman, B. C. Gates, *Angew. Chem.* **2003**, *115*, 714; *Angew. Chem. Int. Ed.* **2003**, *42*, 690; b) A. Comas-Vives, C. Gonzalez-Arellano, A. Corma, M. Iglesias, F. Sanchez, G. Ujaque, *J. Am. Chem. Soc.* **2006**, *128*, 4756.
[6] X. Zhang, H. Shi, B. Q. Xu, *Angew. Chem.* **2005**, *117*, 7294; *Angew. Chem. Int. Ed.* **2005**, *44*, 7132.
[7] a) A. Hoffmann-Röder, N. Krause, *Org. Biomol. Chem.* **2005**, *3*, 387; b) P. Pyykkö, *Angew. Chem.* **2004**, *116*, 4512; *Angew. Chem. Int. Ed.* **2004**, *43*, 4412, and references therein.
[8] a) D. E. De Vos, B. Sels, *Angew. Chem.* **2005**, *117*, 30; *Angew. Chem. Int. Ed.* **2005**, *44*, 30; b) C. J. Jones, D. Taube, V. R. Ziatdinov, R. A. Periana, R. J. Nielsen, J. Oxgaard, W. A. Goddard III, *Angew. Chem.* **2004**, *116*, 4726; *Angew. Chem. Int. Ed.* **2004**, *43*, 4626.
[9] Z. Liu, M. D. Amiridis, Y. Chen, *J. Phys. Chem. B* **2005**, *109*, 1251.
[10] a) A. Eichler, *Phys. Rev. B* **2005**, *71*, 125418; b) A. Christensen, E. A. Carter, *Phys. Rev. B* **1998**, *58*, 8050.
[11] a) J. M. Soler, E. Artacho, J. D. Gale, A. Garcia, J. Junquera, P. Ordejon, S. Portal, *J. Phys. Condens. Matter* **2002**, *14*, 2745; b) N. Troullier, J. L. Martins, *Phys. Rev. B* **1991**, *43*, 1993; c) J. P. Perdew, K. Burke, M. Ernzerhof, *Phys. Rev. Lett.* **1996**, *77*, 3865.
[12] a) Z. P. Liu, X. Q. Gong, J. Kohanoff, C. Sanchez, P. Hu, *Phys. Rev. Lett.* **2003**, *91*, 266102; b) Z. P. Liu, P. Hu. A. Alavi, *J. Am. Chem. Soc.* **2002**, *124*, 14770.
[13] K. Reuter, M. Scheffler, *Phys. Rev. B* **2001**, *65*, 035406.
[14] Z. P. Liu, S. J. Jenkins, D. A. King, *J. Am. Chem. Soc.* **2004**, *126*, 10746.
[15] Breaking of the Au–O_{latt} bond was reported experimentally in CO oxidation on cationic Au/zeolite: J. C. Fierro-Gonzalez, B. C. Gates, *Langmuir* **2005**, *21*, 5693.

